Geoderma xxx (2011) xxx–xxx

Contents lists available at ScienceDirect

Geoderma

journal homepage: www.elsevier.com/locate/geoderma

Field-scale spatial variability of saturated hydraulic conductivity on a recently constructed artificial ecosystem

Willis Gwenzi [a,b,*], Christoph Hinz [a], Karen Holmes [c,d], Ian R. Phillips [e], Ian J. Mullins [a]

[a] School of Earth and Environment (M087), The University of Western Australia, 35 Stirling Highway Crawley, WA 6009, Australia
[b] School of Plant Biology, The University of Western Australia, 35 Stirling Highway Crawley, WA 6009, Australia
[c] Centre of Excellence for Ecohydrology, School of Environmental Systems Engineering, The University of Western Australia, 35 Stirling Highway Crawley, WA 6009, Australia
[d] Department of Agriculture and Food Western Australia, 3 Baron-Hay Court, South Perth WA 6151, Australia
[e] Alcoa of Australia, Pinjarra, Australia

ARTICLE INFO

Article history:
Received 12 November 2010
Received in revised form 7 June 2011
Accepted 21 June 2011
Available online xxxx

Keywords:
Engineered covers
Geostatistics
Hazardous wastes
Recently constructed artificial ecosystems
Saturated hydraulic conductivity
Spatial variability

ABSTRACT

Saturated hydraulic conductivity (K_s) influences water storage and movement, and is a key parameter of water and solute transport models. Systematic field evaluation of K_s and its spatial variability for recently constructed artificial ecosystems is still lacking. The objectives of the present study were; (1) to determine saturated hydraulic conductivity of an artificial ecosystem using field methods (Philip–Dunne, and Guelph permeameters), and compare their results to the constant-head laboratory method; (2) to evaluate the spatial variability of K_s using univariate and geostatistical analyses, and (3) to evaluate the ability of five pedotransfer functions to predict K_s. The results showed that K_s varied significantly ($p<0.05$) among methods, probably reflecting differences in scales of measurement, flow geometry, assumptions in computation routines and inherent disturbances during sampling. Mean K_s values were very high for all methods (38.6–77.9 m day^{-1}), exceeding values for natural sandy soils by several orders of magnitude. The high K_s values and low coefficients of variation (26–44%) were comparable to that of well-sorted unconsolidated marine sands. Geostatistical analysis revealed a spatial structure in surface K_s data described by a spherical model with a correlation range of 8 m. The resulting kriged map of surface K_s showed alternating bands of high and low values, consistent with surface structures created by wheel tracks of construction equipment. Vertical K_s was also spatially structured, with a short correlation range of 40 cm, presumably indicative of layering caused by post-construction mobilization and deposition of fine particles. K_s was linearly and negatively correlated with dry soil bulk density (ρ_b) ($r^2=0.73$), and to a lesser extent silt plus clay percentage ($Si+C$) ($r^2=0.21$). Combining both ρ_b and $Si+C$ significantly ($p<0.05$) improved the relationship and gave the best predictor of K_s ($r^2=0.76$). However, evaluation of five PTFs developed for natural soils showed that they all underestimated K_s by an order of magnitude, suggesting that application of water balance simulation models based on such PTFs to the present study site may constitute a bias in model outputs. Overall, the study demonstrated the influence of material handling, construction procedures and post-construction processes on the magnitude and spatial variability of K_s on a recently constructed artificial ecosystem. These unique hydraulic properties may have profound impacts on soil moisture storage, plant water relations and water balance fluxes on artificial ecosystems, particularly where such landforms are intended to restore pre-disturbance ecological and hydrological functions.

1. Introduction

Hazardous wastes from mining operations and mineral processing pose substantial environmental and public health risks. A key strategy to minimize the migration of pollutants is the use of engineered covers (Albright et al., 2006; Bohnhoff et al., 2009; Ogorzalek et al., 2008). Covers are designed to serve multiple purposes, which include supporting a stable vegetation community that closely resembles natural ecosystems and minimizing deep drainage into buried wastes, both by enhancing soil moisture storage in the top layers, and increasing transpiration and evaporation (Ogorzalek et al., 2008).

Cover construction involves encapsulating the hazardous wastes in single or multiple layers of non-reactive material, followed by establishment of vegetation (Breshears et al., 2005). The nature of materials used for cover construction vary considerably, but locally available materials such as non-reactive overburden material and rock wastes from mineral processing are often used. In contrast to natural ecosystems, such artificially constructed ecosystems can exhibit unique material properties and hydrology. Hydraulic properties,

* Corresponding author at: School of Earth and Environment (M087), The University of Western Australia, 35 Stirling Highway Crawley, WA 6009, Australia. Tel.: +61 8 6488 3735; fax: +61 8 6488 1050.
E-mail address: gwenzw01@student.uwa.edu.au (W. Gwenzi).

0016-7061/$ – see front matter © 2011 Published by Elsevier B.V.
doi:10.1016/j.geoderma.2011.06.010

particularly saturated hydraulic conductivity K_s and soil moisture retention, exert a strong influence on soil moisture storage, deep drainage, runoff and infiltration. Therefore, accurate knowledge of K_s and its spatial variability is crucial for understanding the hydrology of artificially constructed ecosystems such as engineered covers, and provides key inputs for most water balance and solute transport models (Swanson et al., 2003; Holländer et al., 2009.

The methods for measuring K_s and its spatial structure are well-known, and substantial literature exists on the topic particularly on natural soils (Reynolds et al., 2002; Sobieraj et al., 2002; Gómez et al., 2005). However, most existing methods for measuring K_s are time-consuming and labour-intensive, thus constraining the acquisition of large K_s datasets required for spatial analysis. The recent development of rapid and inexpensive K_s field methods such as the Philip–Dunne permeameter (Muñoz-Carpena et al., 2001; 2002) enables acquisition of datasets of appropriate size for geostatistical analysis of K_s spatial patterns.

Geostatistics has been widely used to investigate spatial variability of soil hydraulic properties on natural and agricultural soils, where coefficients of variation as high as 100 to 400% have been reported (Bagarello and Sgroi, 2004; Johnston et al., 2009). Q2 Studies have also shown that K_s values vary considerably among measurement methods (Muñoz-Carpena et al., 2002; Reynolds et al., 2000). Accordingly, Reynolds et al. (2000) proposed that alternative methods for K_s measurement should be evaluated against established procedures such as the constant-head method before use. This is particularly pertinent for the Philip–Dunne field permeameter prototype developed by Muñoz-Carpena et al. (2001) based on the T. Dunne apparatus (Philip, 1993), which has been subjected to limited field evaluation and application.

Land use practices such as forestry, grazing, agriculture and mining have considerable impacts on the magnitude and spatial variability of hydraulic properties (e.g. Bormann and Klaassen, 2008; Breshears et al., 2005; Buczko et al., 2001). In contrast to the substantial literature available on K_s for natural soils (e.g. Botros et al., 2009; Gómez et al., 2005; Sobieraj et al., 2002), there has been no systematic field evaluation of K_s and its spatial variability for artificially constructed ecosystems such as engineered covers. The few studies conducted on mine waste disposal facilities or artificial catchments are based on indirect methods involving analysis of qualitative data on soil structure (Breshears et al., 2005; Buczko et al., 2001), while results of spatial analysis are often not reported probably due to small sample sizes that restrict such analysis (Gerwin et al., 2009; Holländer et al., 2009; Mazur et al., 2011; Wehr et al., 2005). Notable exceptions are two studies conducted in Germany, where geostatistical analysis of hydraulic parameters derived from pedotransfer functions developed for natural soils showed that particle segregation during transportation and dumping, and amelioration practices contributed to spatial variability on lignite mine spoils (Buczko et al., 2001; Buczko and Gerke, 2005). A dye tracer study conducted on covers in New Mexico, USA, a decade after installation showed that macropores caused by root intrusion and fauna enhanced drainage (Breshears et al., 2005). Other studies have evaluated the K_s of synthetic geomembranes and clay liners used as hydraulic barriers (e.g. Albright et al., 2006), and flow mechanisms on highly heterogeneous mine material (e.g. Webb et al., 2008). Most of the existing water balance modeling studies for engineered covers rely on K_s estimated from pedotransfer functions (PTFs) derived for natural soils or few point measurements which fail to characterize the spatial heterogeneity of the site (e.g. Bohnhoff et al., 2009; Ogorzalek et al., 2008). Comparative hydrological prediction of the artificial Chicken Creek using ten different models clearly demonstrated the impact of hydraulic properties and their estimation on water balance components (Holländer et al., 2009).

In summary, analysis of existing studies suggests that K_s integrates numerous complex interactions between the material properties, material handling and construction procedures and the effects of biological activities such as biointrusion and macroporosity (Breshears et al., 2005; Buczko et al., 2001; Buczko and Gerke, 2005; Webb et al., 2008). As the application of 2-D and 3-D water balance and solute transport models becomes increasingly common, it is critical to account for K_s spatial variability in both horizontal and vertical directions. Moreover, until now, studies evaluating the capacity of existing PTFs to predict saturated hydraulic conductivity for artificial material such as bauxite residue sand have been lacking. To address this knowledge gap, the present study applies univariate and spatial statistical analyses to evaluate the variability of K_s on an engineered cover as an example of a recently constructed artificial ecosystem. The specific objectives were; (1) to determine saturated hydraulic conductivity using a combination of in-situ methods (Philip–Dunne and Guelph permeameters) and compare their results to the well-established constant-head laboratory method, (2) to evaluate the ability of five prominent PTFs (Cosby et al., 1984; Dane and Puckett, 1994; Dane and Puckett, 1994; Jabro, 1992; Saxton et al., 1986) to Q3 predict K_s measured by the constant-head method, and (3) to evaluate the horizontal and vertical spatial variability of saturated hydraulic conductivity.

2. Materials and methods

2.1. Description of the study site

The study was conducted on Alcoa (Australia)'s Kwinana Bauxite Residue Disposal Area (RDA), about 35 km to the southwest of Perth, Western Australia. The site experiences a Mediterranean-type climate characterized by cool wet winter (mean annual rainfall: 742 mm) and hot to warm dry summer seasons. In Western Australia, Alcoa operates one of the world's largest integrated bauxite mines, refineries and smelters, contributing about 15% of the world's alumina. Alumina is extracted from the bauxite by the Bayer process. The waste material from the refinery is pumped to a settling column at the RDA where it is separated into red mud (<150 μm in diameter) and residue sand (>150 μm).

The Kwinana RDA was constructed in a series of lifts, whereby the residue sand was either hydraulically poured or hauled to the residue disposal area and used to construct and stabilize tailings dam embankments with a slope of about 1:6. The red mud, which is highly caustic (pH = 12.5), and has high electrical conductivity (60.8 dS m^{-1}) and exchangeable sodium (28 000 mg kg^{-1}) (Courtney and Timpson, 2005; Woodard et al., 2008), is discharged into the tailings dam as slurry or dry staked.

Several studies conducted at Alcoa's Kwinana and Pinjarra residue disposal areas have shown that bauxite residue sand has virtually no organic matter (Eastham et al., 2006; Gherardi and Rengel, 2001). Total organic carbon determined by wet oxidation using the Walkley–Black ranged from about 0.009% in freshly deposited residue sand to 0.09% on 4-year-old rehabilitated sites (Eastham et al., 2006; Gherardi and Rengel, 2001). To enhance vegetation establishment, about 2.25 t gypsum ha^{-1} were applied and mixed to a depth of 150 cm to reduce soil pH and soluble alkalinity. A diammonium-based fertilizer (2.75 t ha^{-1}) was mixed in the top 20 cm-depth to improve soil nutrient status (Gwenzi et al., 2011).

A mixture of tree and shrub species dominated by *Acacia rostellifera* and *Melaleuca nesophila*, and other species endemic to coastal dune ecosystems of Western Australia were established from seedlings and by direct seeding. The site used for this study was established in 2004 and had an average stem density of about 189 plants ha^{-1} at the time of data collection in 2008 (Gwenzi et al., 2011).

Fig. 1(a) is an aerial photo of the study site showing vegetation of different ages and surface structures created by vehicular equipment during material placement and construction. Fig. 1(b) depicts a typical cross-section of the RDA indicating the different layers of gypsum-

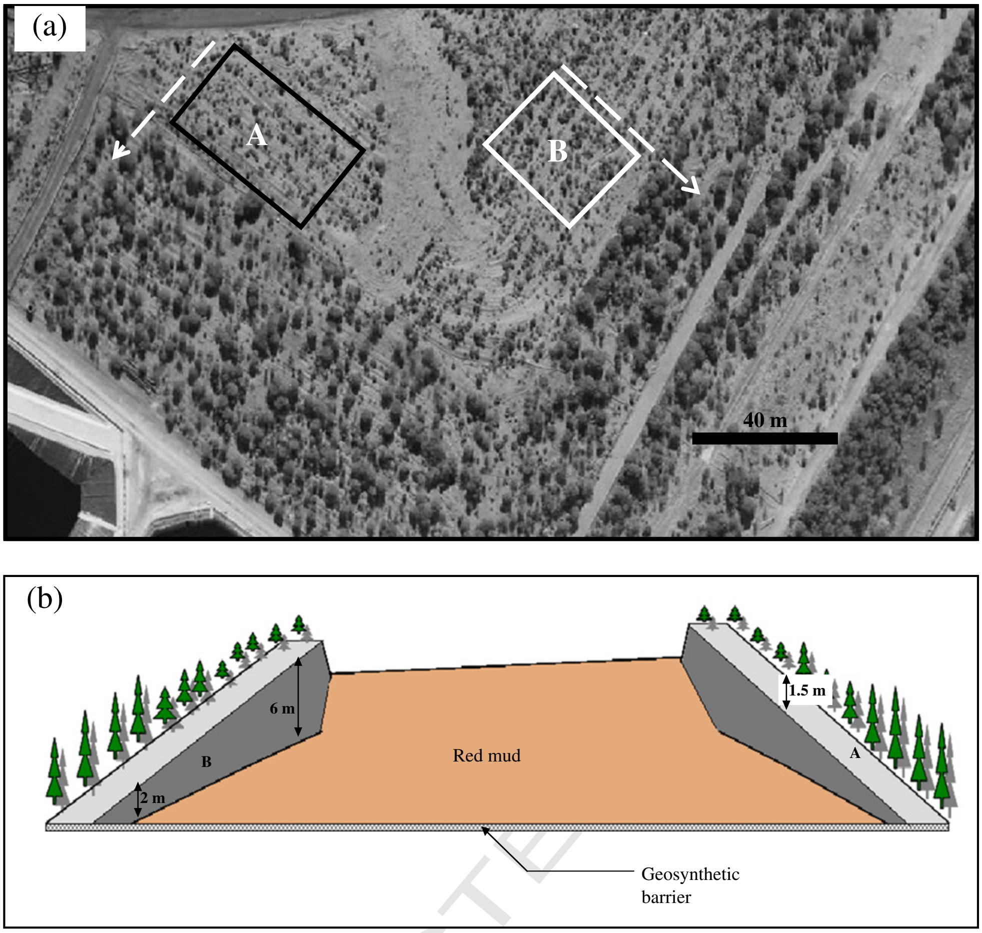

Fig. 1. (a): An aerial photo of a vegetated engineered cover at Kwinana Bauxite Residue Disposal Area. A: surface structures created by wheel tracks during construction and material placement run across the main slope indicated by arrows. B: Location of the sampling site. (Imagery: Google Earth 8 May, 2008; coordinates of lower left corner: 32 12′31″S, 115 49′ 38″E). (b): Sketch of the cross-section of the residue disposal area indicating vegetation of different ages on the embankment. A: gypsum-amended bauxite residue sand, B: unamended alkaline bauxite residue sand, C: red mud core, D: red mud disposed in tailings dam and E: geosynthetic membrane. Note: diagram not to scale. (For interpretation of the references to color in this figure legend, the reader is referred to the web version of this article.)

amended residue sand, unamended residue sand and red mud. The refinery processes, the nature of rock wastes and the disposal practices at the study site bear close resemblance to the current common practices for the disposal of bauxite residues in other parts of the world (Courtney and Timpson, 2005; Woodard et al., 2008).

2.2. Measurement of surface saturated hydraulic conductivity

Two methods were used to measure saturated hydraulic conductivity on a 56-m long × 28-m wide plot within the RDA; Philip–Dunne (PD) permeameter and constant-head (CH) method. Field saturated hydraulic conductivity was measured using a Philip–Dunne permeameter (Muñoz-Carpena et al., 2002) using a 4 m × 4 m grid sampling scheme, giving a total of 112 data points (Fig. 2). To account for spatial variability at lower spatial scales, an additional 45 nested measurements were taken at 2 m, 1 m and 0.5 m at random azimuths from a subset of the gridded sampling points.

The design of the Philip–Dunne permeameter, field protocol and the computation of K_s followed the detailed procedure in literature (Muñoz-Carpena et al., 2001; Muñoz-Carpena et al., 2002; Muñoz-Carpena and Álvarez-Benedí, 2002). A 10-cm diameter auger was used to make a 10 cm deep hole at each sampling point. The permeameter was inserted into the auger hole and filled with water to the 30 cm mark. Initial and final soil moisture was measured for each point using a calibrated theta probe (Model: Delta T Devices). Time required for water level to drop to the 15-cm and 30-cm marks was monitored. Saturated hydraulic conductivity (K_s-PD) was computed using an automated computer routine (Muñoz-Carpena and Álvarez-Benedí, 2002) based on the analysis of Philip (1993). In summary, saturated hydraulic conductivity (K_s) was calculated as:

$$K_s = \left(\frac{\pi^2 r_o \tau_{max}(a)}{8 t_{max}}\right)$$

Where r_o is the radius of a spherical water supply equivalent to half the internal radius of a permeameter, a is a parameter accounting for soil and permeameter characteristics, t_{max} is the time required for the permeameter to empty, and τ_{max} is a nondimensional variable for time calculated from t_{max} (See Appendix 1 for details).

Samples were also collected for laboratory determination of saturated hydraulic conductivity using the core method (K_s-CH) to evaluate whether the PD and core methods give K_s of similar orders of magnitude. A total of 60 core samples were collected a few centimeters from the K_s-PD measurement points using metal cylinders (7 cm diameter × 7 cm height). To minimize sample disturbance, two cylinders were taped together and gently driven into the soil until the lower cylinder was flush with soil. The cylinders and the intact soil cores were carefully taken out. The lower cylinder with intact soil was capped, properly labeled and transported to the laboratory for analysis.

Please cite this article as: Gwenzi, W., et al., Field-scale spatial variability of saturated hydraulic conductivity on a recently constructed artificial ecosystem, Geoderma (2011), doi:10.1016/j.geoderma.2011.06.010

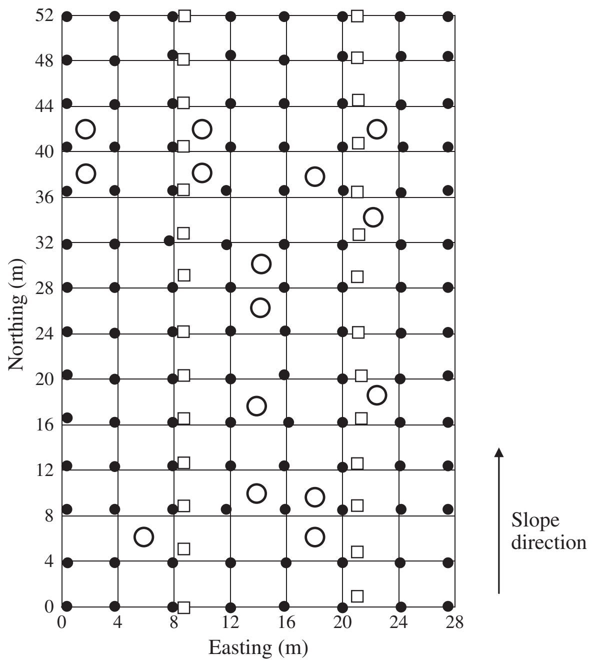

Fig. 2. Grid design showing sampling locations for surface saturated hydraulic conductivity at Kwinana Bauxite Residue Disposal Area. ●: Philip–Dunne (PD), □: constant-head (CH) and ○: a set of three nested samples at 2, 1 and 0.5 m measured using CH.

2.3. Measurement of saturated hydraulic conductivity down profile

To investigate the spatial variability of K_s at depth, additional measurements were conducted in the open face of a 10-m long × 3-m deep trench. Soil cores were collected as described previously at 15 cm and 50 cm-intervals in the vertical and horizontal directions respectively to a depth of 90 cm. Thereafter, the sampling interval was increased to 30 and 100 cm intervals in vertical and horizontal directions, respectively. Since the use of the PD method is in practice limited to a maximum depth of about 15 cm due to the height of the permeameter and difficulties in augering into an unstable trench wall, core samples were supplemented with replicated (4) Guelph permeameter K_s measurements (K_s-GP) at 15 cm intervals up to 3 m for comparison purposes. The Guelph Permeameter (GP) method is one of the most widely applied in-situ methods for determining field saturated hydraulic conductivity (Bagarello, 1997). The method involves augering a small, vertical, cylindrical well and determining the steady water discharge, when a constant depth of water is maintained in the well (Bagarello, 1997). However, because both the PD and GP require augering, the methods could not be used to collect a large K_s data on unstable trench walls at the study site.

Saturated hydraulic conductivity (K_s, m day^{-1}) for the Guelph permeameter was calculated according to Reynolds and Elrick (2002):

$$K_s = \frac{CQ_s}{2\pi H^2 + C\pi a^2 + 2\pi H / a^*}$$

Where C is a dimensionless shape factor that can be calculated from empirical expressions (Reynolds et al., 2002; Zhang et al., 1998):

$$C = \left[\frac{H}{2.074a + 0.093H}\right]^{0.754} \quad \text{for}\, a^* \geq 9\ \text{m}^{-1},$$

Q_s is quasi-steady flow rate out of the permeameter and into the soil (m^3 day^{-1}), H is ponded depth of water or pressure head (m), a is radius of well (m) and a^* is a soil-texture/structure parameter (=36 m^{-1} for coarse and gravelly sands).

2.4. Laboratory analysis

In the laboratory, core samples were analyzed for saturated hydraulic conductivity (K_s-CH), dry soil bulk density (ρ_b) and particle size distribution (PSD). K_s-CH was determined by the constant-head method (Reynolds et al., 2002). A 200 μm nylon mesh was tightly secured to the bottom of the cylinder with intact core samples using a rubber band. To prevent disturbance of the soil surface, a filter paper was put on top of each core, and a second metal cylinder tightly secured to act as a reservoir. Samples were saturated from the bottom in a water bath filled with deionized water for 48 h. K_s was measured using a system consisting of a raised water tank that delivered water at a constant-head of about 3 cm to the core reservoirs. The mass of water eluted from each core was monitored by electronic balances connected to a computer configured to record mass and time. Darcy's law was used to compute saturated hydraulic conductivity (K_s, m day^{-1}) (Reynolds et al., 2002):

$$K_s = -\left(\frac{Q_s dl}{Adh}\right),$$

Where Q_s is water flow rate (m^3 day^{-1}), A is cross-sectional area of flow (m^2), dl is thickness of soil column (m) and dh is hydraulic head (m).

At the end of the K_s measurements, the samples were retained for the determination of dry soil bulk density and particle size distribution. First, core samples were oven-dried at 102 °C for 24 h. The oven dry mass and total soil volume were used to compute dry soil bulk density (Blake and Hartge, 1986). Total porosity (n) was calculated as: $n = 1 - \frac{\rho_b}{\rho_s}$, where ρ_b is the dry bulk density of the sample (kg m^{-3}), and ρ_s is the particle density assumed to be 2650 kg m^{-3}.

Particle size analysis was determined by a combination of sieving and sedimentation (Gee and Bauder, 1986). Soil was dispersed by adding sodium hexametaphospate followed by mechanical shaking. The dispersed suspension was sieved through a 50 μm sieve to separate sand from silt and clay. Silt and clay in the suspension were determined by sedimentation using the pipette method. Soil moisture characteristic curves were determined on core samples using Tempe cells (SOILMOISTURE Equipment Corp, Santa Barbara, CA) for low pressures (0–100 kPa) and pressure plate method for 300 and 1500 kPa (Klute and Dirksen, 1986). The van Genuchten moisture retention model was fitted to the measured data using a nonlinear least squares routine in RETC (van Genuchten, et al., 1991).

2.5. Evaluation of pedotransfer functions

To evaluate the ability of empirical pedotransfer functions (PTFs) to estimate saturated hydraulic conductivity, measured values were compared to those predicted by the PTFs. Our selection of PTFs focussed on those that have been evaluated in previous studies (Sobieraj et al., 2001; Tietje and Hennings, 1996), and availability of input data obtained from field measurements (per cent sand (Sa), silt (Si), clay (C), dry soil bulk density (ρ_b) and saturated soil moisture (θ_s). The PTFs and their input data are presented in Table 1.

2.6. Univariate and geostatistical analyses

Univariate statistical analysis of the data was done in three stages; (1) each dataset was tested for normality and homogeneity (or equality) of variance using the Kolmogorov–Smirnov and Levene tests, respectively. In cases where data were not normally distributed, data transformations were attempted; (2) global summary statistics such as mean, kurtosis, skewness and coefficient of variation (CV) were computed; and (3) for each dataset, a two sample t-test at the 95% probability level was used to compare mean K_s between methods.

Please cite this article as: Gwenzi, W., et al., Field-scale spatial variability of saturated hydraulic conductivity on a recently constructed artificial ecosystem, Geoderma (2011), doi:10.1016/j.geoderma.2011.06.010

Table 1
Pedotransfer functions (PTFs) used to estimate saturated hydraulic conductivity (K_s). Input parameters for the PTFs are sand (Sa): 50–2000 μm, silt (Si): 2–50 μm and clay (C): <2 μm, dry soil bulk density (ρ_b) and saturation soil moisture content (θ_s).

Reference	Pedotransfer function	Inputs
1. Cosby et al. (1984)	$K_s = 25.4 \times 10(-0.6 + 0.012Sa - 0.0064C$	Sa and C
2. Jabro (1992)	$K_s = 9.56 - 0.81\log(Si) - 1.09\log(C) - 4.64\rho_b$	Si, C and ρ_b
3. Puckett et al. (1985)	$K_s = 156.96\exp[-0.19575\,C]$	C
4. Dane and Puckett (1994)	$K_s = 303.84\exp[-0.144\,C]$	C
5. Saxton et al. (1986)	$K_s = 10\exp[12.012 - 0.0755Sa + (-3.895 + 0.03671Sa - 0.1103\,C + 0.00087546(C)^2)/\theta_s]$	Sa, C and θ_s
	$\theta_s = 0.332 - 0.0007251Sa + 0.1276\log10C$ or measured (=0.3)	

Given that K_s measurements were not carried out on exactly the same soil sample or location, a point to point comparison was not feasible, thus comparison of K_s methods was limited to global summary statistics. Regression and correlation analyses were used to test the relationship between K_s estimated by different methods, and the dependence of K_s on dry soil bulk density, sand (Sa), silt (Si) and clay (C). To evaluate PTF performance, predicted K_s values were statistically compared to those measured by the constant-head method. Since K_s dataset measured by the constant-head method deviated from normality, non-parametric statistical tests (Krustal–Wallis) were used for statistical comparison using the median as a measure of central tendency. In all cases, XLSTAT package (Addinsoft, 2009) was used for univariate statistical analysis at 95% probability level.

Geostatistical software GSLIB (Deutsch and Journel, 1998) was used for spatial analysis. Only surface K_s-PD and trench K_s-CH were analyzed for spatial patterns because of the large sample sizes required. Preliminary analysis showed trends in the E–W direction perpendicular to the slope for surface data, and in the vertical direction for the trench data. Directional variogram models were visually fitted to the experimental variograms. For the surface data, a search neighborhood with the following characteristics was used; lag: 3 m, lag tolerance: 3 m, azimuth tolerance: 22.5° and bandwidth: 25 m. A different search neighborhood (lag: 35 cm, lag tolerance: 20–25 cm; azimuth tolerance: 30°, bandwidth: 35–55 cm) was used for the trench data, where sample points were closer together.

The nugget ratio (R) expressed as nugget variance to total variance was used as an indicator of spatial dependence. Spatial dependence was classified as strong if R<25%, moderate if 25%<R<75%, weak if R>75% (Cambardella et al., 1994). If the slope of the variogram was close to zero, K_s was considered randomly distributed. In cases where spatial patterns were detected, the variograms were incorporated in a kriging routine to map K_s spatial distribution.

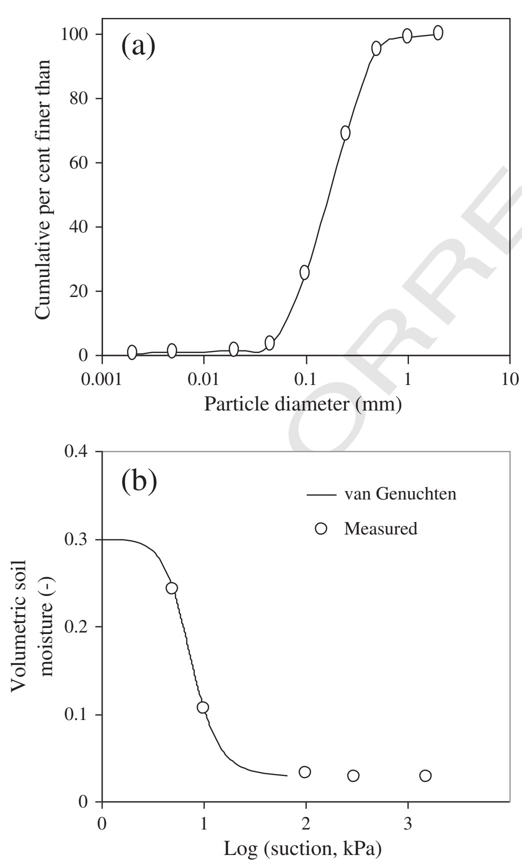

Fig. 3. (a) Semi-logarithmic plot of particle size distribution. The y-axis is linear while x-axis is in logarithmic scale. (b) Soil moisture characteristic curve for bauxite residue sand showing measured points (dots) and fitted van Genuchten function (solid line). The van Genuchten parameters related to air-entry value ($\alpha = 0.15$ kPa^{-1}) and pore size distribution ($n = 3.58$) were estimated by RETC (version 6.02) (van Genuchten, et al., 1991).

3. Results

The cover material had a well-sorted predominantly sandy texture (96%) with very low silt plus clay fraction (Fig. 3a). As expected, soil moisture retention was very low (10.1% at 10 kPa and 2.8% at 1500 kPa) as evidenced by a sharp drop in soil moisture within suction ranges of 0–100 kPa (Fig. 3b).

Mean K_s values were very high for all methods (38.7–77.9 m day^{-1}) (Table 2). The K_s data were slightly negatively skewed, with the exception of K_s-PD, which was positively skewed. Kolmogorov–Smirnov normality tests (Table 2), frequency distribution curves and probability–probability plots showed that surface K_s for both methods conformed to a normal distribution (Figs. 4a and b and 5a and b), while trench data deviated significantly from normality (p>0.05) and had a tendency to exhibit a bimodality (Figs. 4c and d and 5c and d). Attempts to normalize the bimodal trench data by transformation had no effect on kurtosis, skewness and results of the Kolmogorov–Smirnov normality test. By inference such data cannot be subjected to parametric statistical analysis. To remedy this, the trench K_s data were split into two sub-populations (0–90 cm and 120–300 cm) which were normally distributed (Figs. 4e and f and 5e and f).

Table 2
Summary statistics of saturated hydraulic conductivity at Kwinana Bauxite. Residue Disposal Area measured by the Philip–Dunne (K_s-PD), constant-head (K_s-CH) and Guelph (K_s-GP) permeameters.

	Surface K_s measurements		Trench K_s measurements	
	K_s-PD	K_s-CH	K_s-GP	K_s-CH
Sample size, n	157	27	28	131
Minimum (m day^{-1})	6.1	23.6	16.1	5.8
Maximum (m day^{-1})	164.9	82	62	116.3
Mean (m day^{-1})	77.9	55	38.6	64.6
Coefficient of variation, CV (%)	44	26	37	41
Skewness	0.56	−0.23	−0.03	−0.52
Kurtosis	−0.12	−0.30	−1.43	−0.65
Kolmogorov–Smirnov test	p<0.05	p<0.05	p>0.05	p>0.05

Please cite this article as: Gwenzi, W., et al., Field-scale spatial variability of saturated hydraulic conductivity on a recently constructed artificial ecosystem, Geoderma (2011), doi:10.1016/j.geoderma.2011.06.010

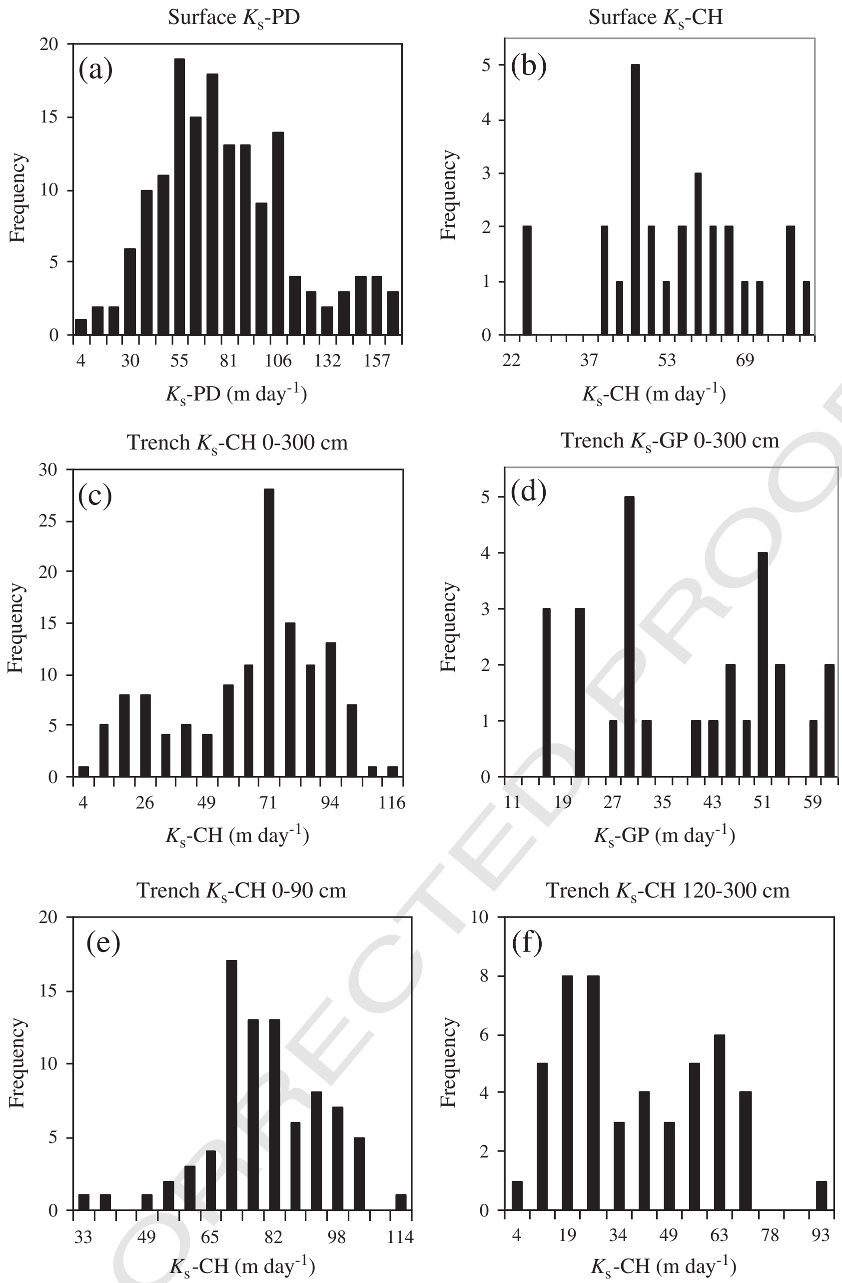

Fig. 4. Histograms for surface (a) and (b) and trench (c)–(f) saturated hydraulic conductivity at Kwinana Bauxite Residue Disposal Area.

Comparison of mean K_s measured in-situ versus laboratory measurements revealed significant ($p<0.05$) differences. For surface measurements, mean K_s-PD (77.9 m day^{-1}) was 1.4 times higher than K_s-CH (55 m day^{-1}), while for the trench measurements mean K_s-CH (64.6 m day^{-1}) was 1.7 times that of K_s-GP (Table 2). However, field and laboratory measured K_s values were linearly correlated ($r^2=0.63$–0.72; $p<0.05$), and in all cases the mean values and coefficients of variation (CV) were within the same orders of magnitude. For the trench measurements, mean K_s-GP fell within the range for K_s-CH except in the top 30 cm (Fig. 6a). The K_s for both methods displayed a similar depth trend characterized by highest K_s in the top 90 cm, and a sharp drop at 120-cm depth (Fig. 6a), almost coinciding with the maximum depth of gypsum incorporation. Overall, K_s dropped with depth, from 51 to 80 m day^{-1} at the surface to 25 m day^{-1} at 300 cm. Dry soil bulk density was generally low throughout the profile, but increased significantly with depth ($p<0.05$, $r^2=0.88$) from about 1350–1400 kg m^{-3} in the top 1 m-depth to about 1500 kg m^{-3} below 1.5 m (Fig. 6b). As expected, mean total porosity (43–50%) also significantly declined with soil depth ($p<0.05$, $r^2=0.86$) (Fig. 6c).

Measured K_s was significantly ($p<0.05$) correlated to dry soil bulk density ($r^2=0.73$), but the relationship with silt plus clay percent was weaker ($r^2=0.21$) (Fig. 7). Multiple regression analysis revealed an inverse linear relationship between measured K_s and the combined effect of dry soil bulk density ρ_b (kg m^{-3}) and silt plus clay percent ($Si+C$). The resulting linear model for saturated hydraulic conductivity (m day^{-1}) ($K_s=551.3-0.3\rho_b-13.6(Si+C)$, $r^2=0.76$) provides a first-order estimate of K_s for the cover. The relationships between K_s, and dry soil bulk density and particle size distribution have been used to develop several pedotransfer functions, which are widely used for predicting K_s (Sobieraj et al., 2001; Tietje and Hennings, 1996). Evaluation of five prominent PTFs based on dry soil bulk density, soil moisture at saturation and percent sand, silt and clay showed that they all underestimated K_s by more than one order of magnitude (Fig. 8). However, the five PTFs (Cosby

Please cite this article as: Gwenzi, W., et al., Field-scale spatial variability of saturated hydraulic conductivity on a recently constructed artificial ecosystem, Geoderma (2011), doi:10.1016/j.geoderma.2011.06.010

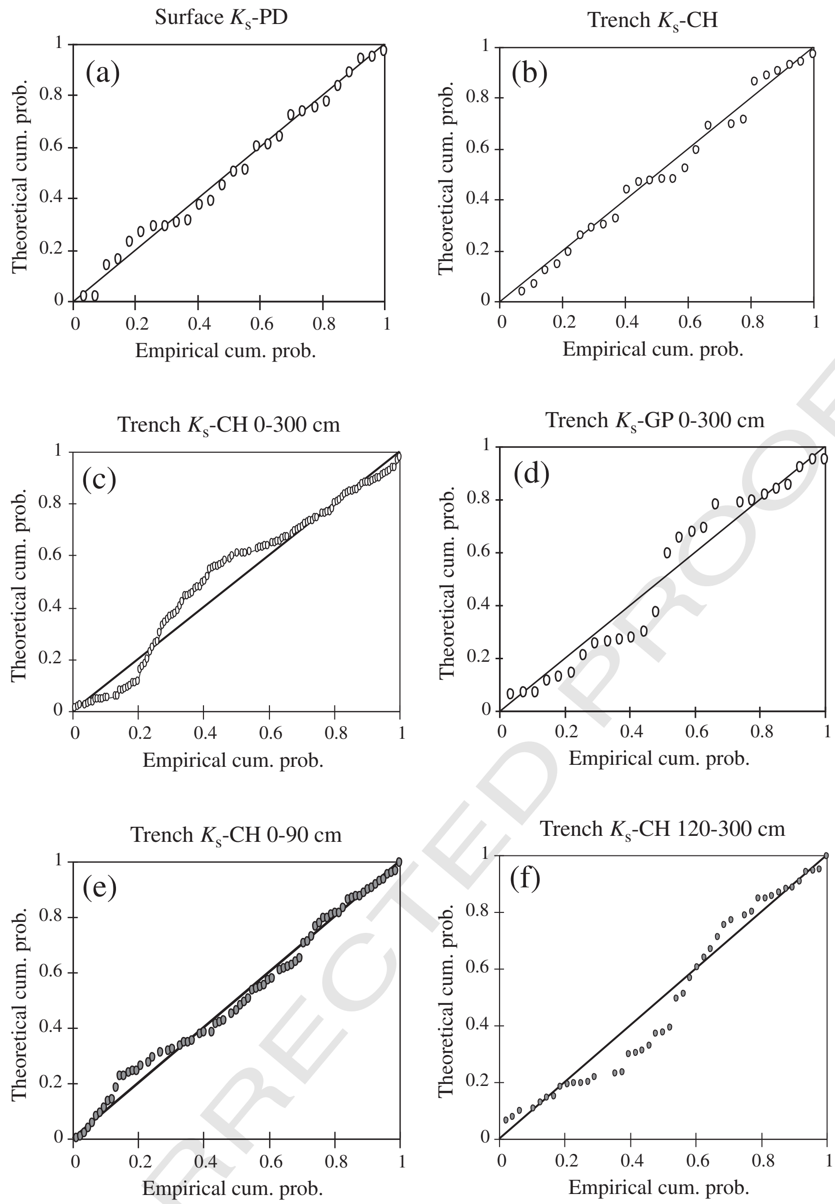

Fig. 5. Cumulative probability–probability plots of surface (a) and (b) and trench (c)–(f) saturated hydraulic conductivity K_s measured by constant-head method (K_s-CH), Guelph permeameter (K_s-GP and Philip–Dunne permeameter (K_s-PD).

et al., 1984; Dane and Puckett, 1994; Jabro, 1992; Puckett et al., 1985; Saxton et al., 1986) predicted comparable K_s values (median: 1.3–3.4 m day^{-1}).

The variogram of surface K_s showed a moderate spatial dependence in the E–W direction perpendicular to the slope (Fig. 9a). The spatial structure was described by a spherical variogram with a correlation range of 8 m and a nugget/sill ratio of 78%. In the N–S direction or downslope, K_s showed a pure nugget effect or no spatial structure. This indicated that K_s exhibited more spatial heterogeneity in the downslope direction (N–S), and less so in the direction parallel to the slope (E–W). For clarity, only the variogram indicating a spatial structure in the direction perpendicular to the slope is shown in Fig. 9a. Considering the strong trend in K_s with depth, and the bimodality of the data (Fig. 5c–d), the final variogram analysis was performed on all data (Fig. 9b), and treating the 0–90 cm and 120–300 cm data separately (Fig. 9c). The vertical trend (linear: $r^2 = 0.52$, $p < 0.01$) was removed from the raw data and variogram models fitted to the residuals, which were normally distributed. There was a strong spatial structure in the vertical direction described by a spherical variogram with a correlation range of 40 cm, and a linear trend parallel to the surface (Fig. 9b). Separating the data into two subsets to account for layering revealed a moderate ($R = 64\%$) spatial structure in the top 90 cm described by a bounded spherical variogram with a range of 2 m (Fig. 9c). A linear variogram best described the K_s data for the 120–300-cm depth. Variability of K_s at 120–300 cm was higher than in the top 90 cm (Fig. 9c). It is worth noting that, compared to the variogram for the 0–90 cm depth, the variogram for the 120–300 cm depth was based on few data points (about 60), which made short-distance spatial relationships difficult to interpret. Variance was higher for the surface measurements than the trench data (Fig. 8a and b). The variogram models were used to interpolate (krige) K_s for the surface and trench data. The map of surface K_s showed distinct alternating bands of relatively high and low K_s running perpendicular to the slope (E–W direction) (Fig. 10). The described vertical trend of a drop in K_s at about 1 m depth (Fig. 9) was captured in the kriged map of trench data (Fig. 11). As represented in the variograms (Fig. 9c), the bottom 120–300 cm for the trench varied more smoothly than the top 90 cm.

Please cite this article as: Gwenzi, W., et al., Field-scale spatial variability of saturated hydraulic conductivity on a recently constructed artificial ecosystem, Geoderma (2011), doi:10.1016/j.geoderma.2011.06.010

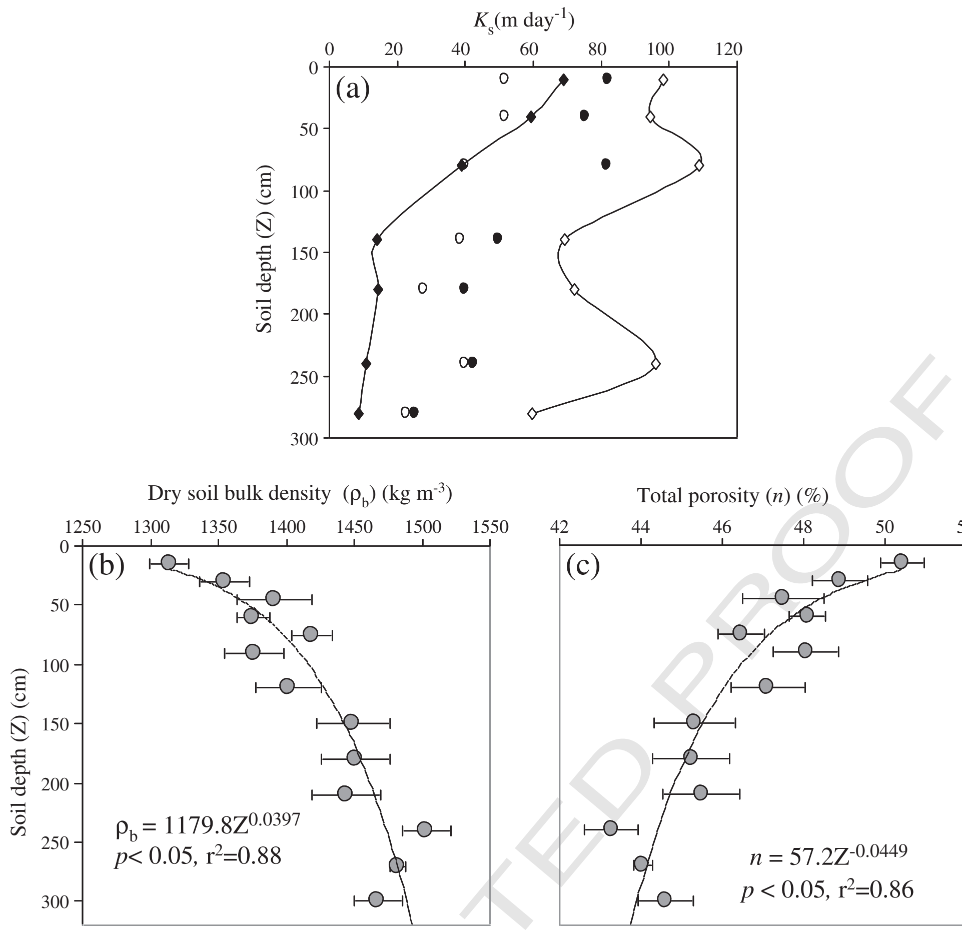

Fig. 6. (a) Depth variation of saturated hydraulic conductivity at Kwinana Bauxite Residue Disposal Area. ◆, ●, ; minimum, mean and maximum saturated hydraulic conductivity measured by the constant-head method. ○: mean saturated hydraulic conductivity measured by Guelph permeameter. (b) Dry soil bulk density and (c) total porosity. Data shown in figures (b) and (c) are means ± standard errors.

4. Discussion

The present study used multiple field and laboratory methods to quantify the range and variability of surface and vertical saturated hydraulic conductivity on a mine waste cover. As observed in earlier studies (e.g. Wehr et al., 2005), soil moisture characteristic curves showed that residue sand had low water retention capacity. The van Genuchten pore size distribution index (n) was 3.58, while α, which is inversely related to the air-entry value was 0.15 kPa^{-1}. The corresponding air-entry value (6.6 kPa) was relatively higher than values reported for natural sandy soils (2.0 to 3.2 kPa) (e.g. Wang et al., 2009; Zhu and Mohanty, 2002), probably due to the fact that our data had very limited measurement points at low suctions (<5 kPa). On the other hand, the high n value indicated a narrow pore size distribution, which reflected the well-sorted particle size distribution shown in Fig. 3(a).

Although K_s values differed among methods, both field and laboratory methods adequately captured the range and variability of K_s at the study site. The low-cost PD permeameter has proven acceptable for rapid acquisition of a large K_s dataset such as required for geostatistical analysis. As observed in previous studies (e.g. Bagarello, 1997; Johnston et al., 2009; Muñoz-Carpena et al., 2002), the imperfect agreement between field and laboratory methods is not surprising. However, the magnitude of variability among methods observed in this study was lower than that reported in literature (Muñoz-Carpena et al., 2002; Reynolds et al., 2000), probably because the previous studies were conducted on structured soils with macropores. The exact causes of discrepancies among methods were beyond the scope of the present investigation, however previous studies attributed similar findings to differences in flow geometry, assumptions in computation routines, sampling volumes and inherent disturbances during sampling (Bagarello, 1997; Johnston et al., 2009; Muñoz-Carpena et al., 2002; Reynolds et al., 2000). For example, surface smearing, compaction of the well surface during augering, sinking of the water outlet tip of the instrument into the base of the well during a measurement, and radius of the well can affect field-saturated hydraulic conductivity measured with the Guelph Permeameter (Bagarello, 1997). Moreover, in our case, because the laboratory method was destructive, it was impossible to measure K_s on exactly the same points or soil sample thus increasing differences observed between measurement methods. Previous studies have also shown that K_s increases as the scale of measurement or sampling volume increases particularly for structured soils with macroporosity (e.g. Bagarello, 1997; Bradbury and Muldoon, 1990). Therefore, small sample volumes may fail to account for K_s arising from macropore or preferential flow (Mallants et al., 1997). Q5 Given that the study material was highly porous, unconsolidated and had no macro-structure, we doubt that core volume or diameter of the field permeameters accounts for the high K_s observed in the present study. The fact that different methods gave similar K_s values further suggests that the observed high K_s values are an intrinsic property of the system.

Univariate analysis revealed two important findings on saturated hydraulic conductivity for artificially constructed ecosystems which deviate from trends observed for natural sandy soils. First, K_s values were very high irrespective of method of measurement. Second, surface K_s conformed to a normal distribution, while trench data were

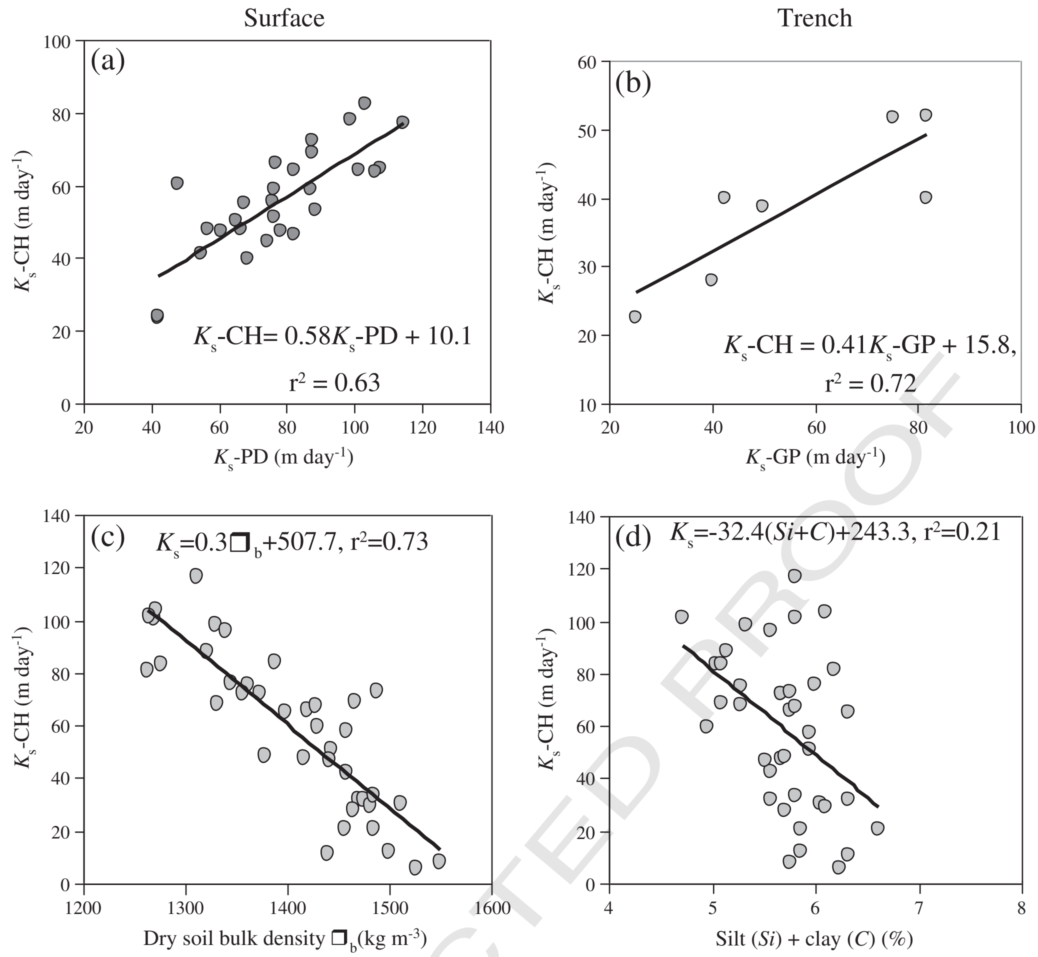

Q12 **Fig. 7.** Correlation between K_s measured by various methods (a) and (b), and between K_s and bulk density (c) and silt (*Si*) plus clay (*C*) percent (d).

bimodal rather than lognormal, as often reported for natural soils (e.g. Botros et al., 2009; Johnston et al., 2009). Dry soil bulk density and total porosity data indicate that the material was unconsolidated and highly porous. Total porosity was higher than 25–35% reported for Q6 sandy dune systems (Salama et al., 2005). Such low dry bulk density and high total porosity values (43–47%) are common in unconsolidated marine sands prior to any diagenesis such as post-depositional cementation and overburden stress (Bennett et al., 2002.

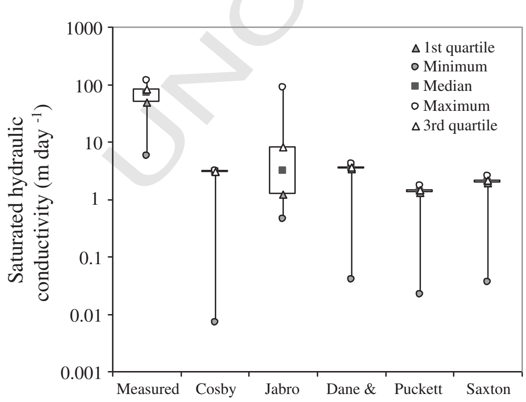

Fig. 8. Box-plot comparison of saturated hydraulic conductivity measured by constant-head method and predicted by five pedotransfer functions (Cosby et al., 1984; Dane and Puckett, 1994; Jabro, 1992; Puckett et al., 1985; Saxton et al., 1986). Note that the y-axis is in logarithmic scale.

The observed K_s values were several orders of magnitude higher than those reported in literature on natural sandy soils and artificial ecosystems, where K_s often exhibits high variability (CV: 100–400%) (Bagarello, 1997; Reynolds et al., 2000; Buczko et al., 2001; Salama et Q7 al., 2005; Botros et al., 2009). For example, observed K_s values were remarkably higher than those reported for deep alluvial sandy soils (0.05–14.5 m day^{-1}) (Botros et al., 2009) and sandy dune systems of the Swan Coastal Plain in Western Australia (0.4–7.3 m day^{-1}) (Salama et al., 2005). Even, sandbank island sediments consisting of Q8 quartz sand had lower K_s values (2.4–3.8 m day^{-1}) Klaassen et al., 2008) than observed in the present study. Moreover, the observed K_s was even much higher than that of other artificial ecosystems such as engineered covers (8.6×10^{-7}–8.6×10^{-1} m day^{-1}) (Bohnhoff et al., 2009; Ogorzalek et al., 2008) and the artificial Chicken Creek catchment (0.2–2.3 m day^{-1}) (Gerwin et al., 2009; Holländer et al., 2009; Mazur et al., 2011). However, most of these studies (e.g. Klaassen et al., 2008) failed to provide information on total porosity, dry soil bulk density, degree of sorting and particle size distribution of the material or sediments.

The high saturated hydraulic conductivity, low spatial variability and low soil moisture retention observed in the present study reflected the unconsolidated and highly porous nature of the material as evidenced by low dry soil bulk density and high total porosity. These properties were attributed to mechanical separation, which resulted in well-sorted coarse-textured material. Moreover, it is also possible that crushing and mechanical milling of hard rock ores could generate angular particles that tend to pack loosely as reported in laboratory and modeling studies of particulate systems (e.g. Latham et al., 2002). Although most studies investigating the hydraulic

Please cite this article as: Gwenzi, W., et al., Field-scale spatial variability of saturated hydraulic conductivity on a recently constructed artificial ecosystem, Geoderma (2011), doi:10.1016/j.geoderma.2011.06.010

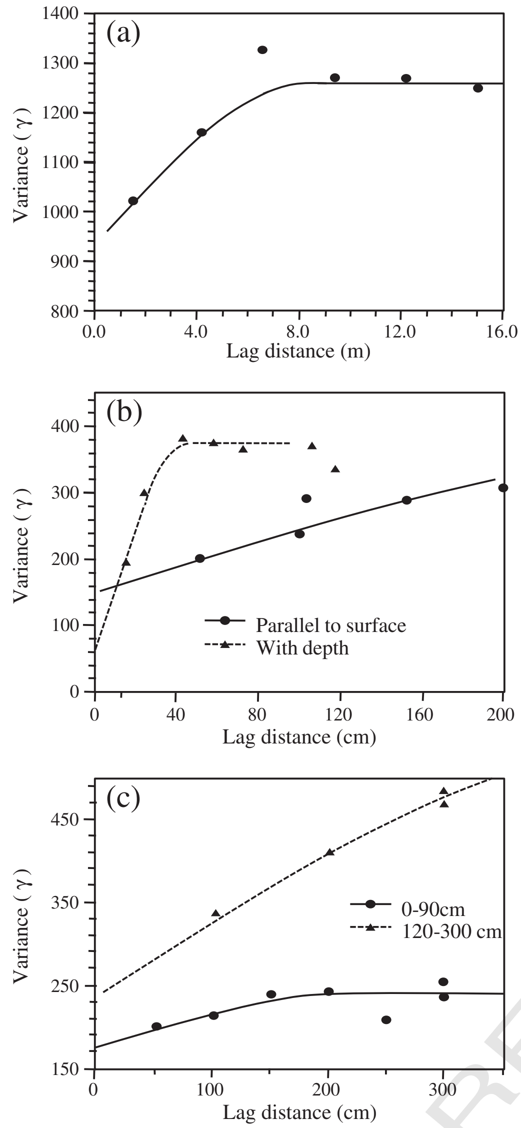

Fig. 9. Directional variograms of saturated hydraulic conductivity K_s. (a) surface, perpendicular to slope at 325 azimuth; (b) trench, residuals from the linear model oriented parallel (horizontal, X) and perpendicular (vertical, Z) to the soil surface ; (c) trench, vertical (Z)-direction for 0–90 cm and 120–300 cm depths.

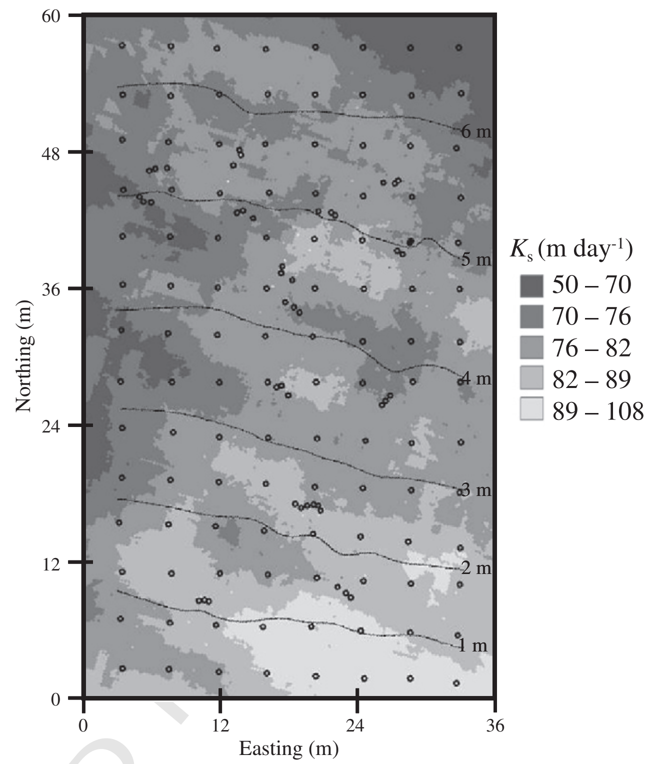

Fig. 10. Kriged map of surface K_s-PD showing surface spatial structure or bands across the N–S slope. Marked points indicate sampling locations.

properties of coastal sands have reported their results in terms of permeability, estimation of K_s from published data on permeability revealed that observed K_s values were comparable to those reported for coastal sands (Wiebenga et al. (1970); Wilson et al., 2008). One similarity between coastal sands subjected to wave action or currents, and mechanically separated bauxite residue sand is the high degree of sorting and poor consolidation that results in a high total porosity and hydraulic conductivity. The impacts of sorting on hydraulic properties and total porosity have been documented in several studies (Forster et al., 2003; Wiebenga et al., 1970; Wilson et al., 2008). Indeed, for well-sorted coastal sediments dominated by fine and coarse quartz sand, K_s values of 17 to 2592 m day^{-1}, and total porosities of 38 to 44% have been reported in literature (e.g. Wiebenga et al., 1970). Similarly, 23 separate studies conducted on well-sorted marine sands reported K_s
Q9 values of 2 to 353 m day^{-1} (Wilson et al., 2008). Besides coastal sands, extremely high K_s spanning four orders of magnitude (<0.57–>500 m day^{-1}) have been reported in coastal floodplain acid sulfate soils with prevalent macropores or preferential pathways (Johnston et al., 2009). However, in the present case, profile observations showed no evidence of profile development and preferential flow pathways.

Correlation analysis showed that dry soil bulk density and particle size distribution accounted for the spatial variability of K_s. Negative correlations between K_s, dry soil bulk density, silt and clay have been observed in several studies and form the basis for the development of pedotransfer functions (Saxton et al., 1986; Sobieraj et al., 2001; Tietje and Hennings, 1996). The inverse relationship between K_s and dry soil bulk density was consistent with the expected effect of overburden stress. However, the five pedotransfer functions evaluated in this study underestimated K_s for the study site. Discrepancies between measured and predicted K_s values have been reported on both natural soils (e.g. Sobieraj et al., 2001; Tietje and Hennings, 1996), artificial Q10
ecosystems (Holländer et al., 2009) and well-sorted marine sands (Wilson et al., 2008). The poor performance of the PTFs observed in the present study may be due to a number of reasons; first, the PTFs were developed based on databases for natural soils, most of which tend to be poorly sorted. For example, a search of the databases used to develop some of the PTFs revealed that no data on artificial ecosystems were included. Moreover, as Tietje and Hennings (1996) observed, very high K_s values are often excluded in datasets used to develop PTFs. Therefore, most of the PTFs evaluated here gave maximum K_s values of about 2 to 10 m day^{-1}. Second, whereas material sorting and angular granular shapes may influence K_s particularly on artificial ecosystems such as covers (e.g. Latham et al., 2002; Wilson et al., 2008), none of these factors are accounted for in the PTFs evaluated here. Accordingly, Wilson et al. (2008) attributed the failure of PTFs to predict either the mean permeability or the variability in well-sorted marine sands to their failure to account for sorting. On the other hand, multiple regression analysis revealed that K_s for bauxite residue sand can be predicted by a simple model incorporating dry soil bulk density and per cent silt plus clay.

The trench data indicated soil layering or stratification, as represented by the frequency distribution curves. The transition zone between the two layers occurred at about 120 cm, which generally coincides with the maximum depth of gypsum incorporation. Gypsum is a strong flocculant, which may reduce the dispersive

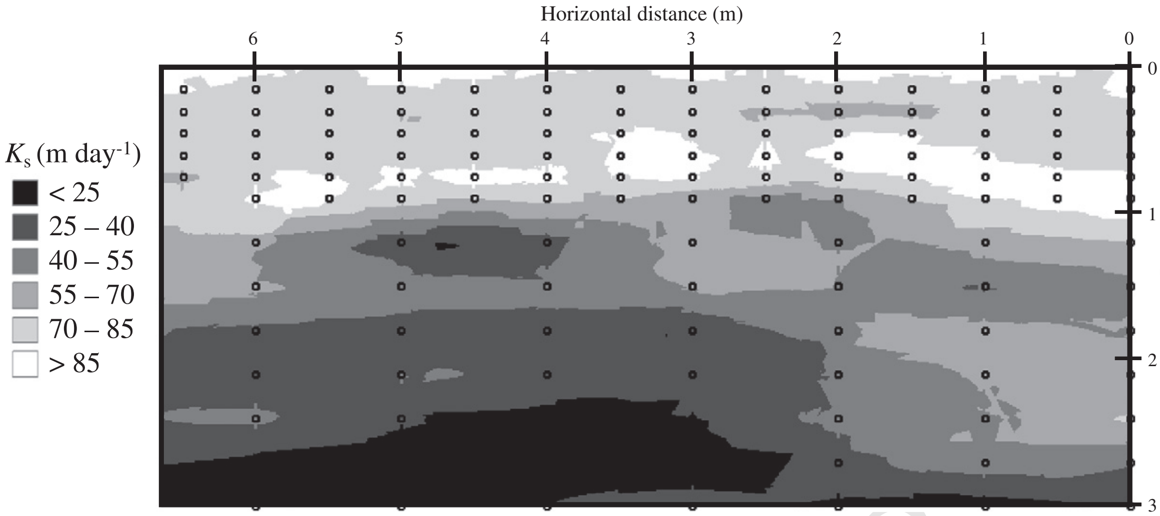

Fig. 11. A kriged map of trench K_s-CH indicating vertical layering. Marked points represent sampling locations.

effects of high exchangeable sodium percentage associated with bauxite residues. Dispersion in samples collected below 120 cm was observed during K_s measurement using the constant-head method. Therefore, it is possible that clay dispersion and subsequent mobilization below 120 cm could have contributed to the layering and increase in dry soil bulk density. Moreover, particle segregation during material handling and dumping has also been reported on coal mine spoils, where both dry soil bulk density and K_s showed depth trend (Buczko et al., 2001). On mine waste materials in Australia, mobilization and self-filtration of fine particles have been reported to reduce K_s through pore clogging (Dikinya et al., 2008). This phenomenon is also well pronounced in coastal sediments, where even small amounts of mud have been reported to clog pore throats, reduce K_s and enhance further deposition of the fine particles (Forster et al., 2003; Wilson et al., 2008). This suggests that the increase in silt and clay with depth may result from mobilization from the top layers and deposition at depth, leaving a skeletal material dominated by the coarse fraction. Although overall K_s will remain high due to the low silt plus clay percentage, it is likely that, over time, K_s of the surface layers may further increase, while that of deeper layers decrease, resulting in a profile comparable to a duplex soil.

Surface K_s was relatively similar across slope and changed more rapidly down slope, as illustrated by the mapped alternating bands of high and low K_s perpendicular to the slope (Fig. 10). The spatial structure was attributed to variability of dry soil bulk density caused by vehicular traffic movement during construction and incorporation of chemical amendments. This explanation is consistent with aerial photo and field observations showing surface structures running perpendicular to the main slope (see Fig. 1). The trench K_s data showed spatial patterns in both vertical and horizontal directions. The correlation range was longer for the surface K_s (8 m) than trench data (0.4–2 m), indicating higher spatial dependence for surface measurements than vertical ones. This finding is in agreement with that of Botros et al. (2009), who reported ranges of 5–8 m in the horizontal direction and 0.5 to 1.5 m in the vertical direction for deep alluvial sediments. Besides differences in sampling intensity, this could be indicative of the different processes influencing K_s in the two directions. Results of spatial analysis of K_s for natural soils reported in literature vary greatly among studies, soil types and sampling scales. Bounded variograms with correlation ranges of 2–6 m have been reported for agricultural soils (Gómez et al., 2005), while other studies showed pure nugget effect or random variation (Sobieraj et al., 2002).

For sampling purposes, the results of spatial analysis suggest that to characterize the variability of K_s, more intensive sampling is required parallel to the slope for surface measurements, and in the vertical direction for trench measurements. Overall, both surface and trench K_s varied with direction as evidenced by distinct directional variograms (surface not shown; vertical: Fig. 9b). The vertical direction variograms exhibited short ranges with a sill for the 0–90 cm depth (Fig. 8b and c), indicative of patchiness and sharp discontinuities (Ettema and Wardle, 2002). The trench horizontal linear variogram increases with lag distance without reaching a sill, describing a smooth regional trend (Ettema and Wardle, 2002) illustrated in the kriged map for trench data for the horizontal direction and 120–300 cm depth.

Overall, our results demonstrated that the study material was unconsolidated and highly porous material, and had unique hydraulic properties, characterized by remarkably high saturated hydraulic conductivity, low variability and low moisture retention resembling that of well-sorted marine sands. Earlier studies on the spatial distribution of fluid flow and hydraulic properties on artificial ecosystems such as mine spoils observed high spatial heterogeneity (e.g. Buczko et al., 2001; Buczko and Gerke, 2005; Webb et al., 2008). Contrary, our findings showed that on material subjected to artificial separation, spatial variability can be very low. Given that the disposal of bauxite residue at the present study site closely resembled the global practice in the alumina industry (Courtney and Timpson, 2005; Woodard et al., 2008), Q11 we infer that the magnitude and spatial variability observed in the present study may be prevalent at other bauxite residue disposal sites. However, considering the diversity of mine spoils and material handling procedures, our results, and those of previous studies (e.g. Buczko et al., 2001; Buczko and Gerke, 2005; Webb et al., 2008) suggest that it is difficult to draw generalized conclusions about the spatial variability of hydraulic properties on artificial ecosystems and stress the need for site-specific field measurements.

5. Implications for hydrology of cover systems

The findings have implications for the hydrological performance, ecosystem functions and modeling of vegetated engineered covers, particularly in water-limited ecosystems. To minimize the risk of deep drainage, an ideal cover system should have the capacity to store moisture in the root-zone for a relatively prolonged period, and deplete it via root water uptake and bare soil evaporation before the storage capacity of the soil is reached. The high K_s and low spatial variability imply rapid downward water movement throughout the profile. We further infer that, given the high K_s values, rainfall input rather hydraulic properties limit saturated flow on such a system.

Consequently, under saturated conditions and during substantial rainfall events, deep drainage may constitute a major water balance component on such a system.

The soil moisture retention curve was characterized by a sharp drop in soil moisture at a low suction of about 10 kPa, reaching a steady state at about 100 kPa suggesting rapid wetting and drying. Coupled with high seasonality of rainfall associated with Mediterranean environments, and a superficial root distribution with approximately 90% of the roots occurring in the top 0.4 cm of the profile, decreasing exponentially to a maximum rooting depth of 1.5 m (Gwenzi et al., 2011), high K_s and low moisture retention imply low moisture storage in the root-zone.

The impact of these hydraulic properties on soil moisture dynamics in the root-zone, plant water stress and vegetation water use has been reported in previous studies (Gwenzi, 2010; Wehr et al., 2005). For instance, long-term (2 years) soil moisture data showed rapid wetting of the whole 90-cm depth within hours after substantial rainfall events, but soil moisture in the root-zone dropped sharply thereafter, indicating rapid drying and potential loss of plant available soil moisture to drainage (Gwenzi, 2010). In the dry summer season, the root-zone remained extremely dry for periods up to three months resulting in severe plant water stress and reduced vegetation water use. An experimental investigation of plant physiological behavior conducted on similar material at Alcan Gove, Northern Territory also showed rapid drying and severe plant water stress (Wehr et al., 2005). Using sap flow sensors, Gwenzi (2010) estimated that the contribution of vegetation water use to the annual water balance of the present study site was quite low (147 mm) and equivalent to 22% of annual total rainfall (693 mm). Therefore, we recommend that material characterized by high K_s and low moisture retention such as bauxite residue sand are not ideal for constructing water balance cover systems particularly in water-limited environments.

Most water balance models rely on pedotransfer functions developed for natural soils to estimate hydraulic properties for artificial ecosystems, yet evaluation of five pedotransfer functions revealed that they all underestimated K_s for the study material. As Holländer et al. (2009) pointed out, such underestimation may have profound effects on moisture storage and, and hence water balance fluxes. Several hydrological modeling studies have clearly demonstrated the impacts of using different PTFs on model outputs and uncertainties (e.g. Holländer et al., 2009; Sobieraj et al., 2001). Therefore, we recommend that direct application of PTFs developed for natural soils on artificial ecosystems should be avoided unless the accuracy of the PTF has been validated.

6. Conclusions

This paper represents the first systematic study to evaluate field-scale spatial variability of saturated hydraulic conductivity on a recently constructed artificial ecosystem. In contrast to natural sandy soils, the cover material was well-sorted and coarse-textured, resulting in very high K_s, low moisture retention and low variability similar to that of well-sorted unconsolidated marine sands. Geostatistical analysis revealed surface spatial patterns of K_s associated with structures created during cover construction, and vertical layering caused by migration and deposition of fine particles. Overall, the magnitude and spatial variability of hydraulic properties reflected the influence of material handling and construction procedures, and post-construction processes. A linear model based on dry soil bulk density and particle size distribution provides a good estimate of K_s for the study site. These findings demonstrate that certain artificially constructed ecosystems can exhibit unique hydraulic properties beyond those expected for natural sandy soils. This has important implications for soil moisture storage, plant water relations and water balance fluxes on recently constructed ecosystems, particularly, where such covers are intended to restore pre-disturbance ecological and hydrological functions. Evaluation of five pedotransfer functions for predicting saturated hydraulic conductivity suggests that application of water balance simulation models based on such PTFs may constitute a major uncertainty in hydrological modeling. Therefore, there is need for caution when using models based on PTFs that have not been validated for artificial ecosystems.

Acknowledgments

We are grateful to the Australian mining industry Covers Project for research funding. The design and implementation of the experiment, and analysis and interpretation of the data were solely the responsibilities of the authors. Scholarship support for WG was provided by The University of Western Australia through the Scholarship for International Research Fees (SIRF), University Postgraduate Award (International Student) (UPAIS) and an Ad-hoc-top-up scholarship. Mr. Johannes Albers assisted with fieldwork and laboratory analysis. We also thank Dr. Rafael Muñoz-Carpena for the Philip–Dunne prototype, the pDunne computer routine for computing saturated hydraulic conductivity and application of the program.

Appendix. Calculation of K_s from the Philip–Dunne permeameter data

The procedure for computing K_s from Philip–Dunne measurements based on Philip (1993) is presented in Muñoz-Carpena et al. (2002). To obtain K_s with the Philip–Dunne permeameter, Philip (1993) applied a spherically symmetric Green and Ampt analysis based on the effective hemisphere model for unsteady state infiltration. For a permeameter of internal radius r_i, Philip (1993) assumed a spherical water supply of radius $r_o = 0.5r_i$. If $R = R(t)$ is the radius of soil-wetted bulb from the water supply at time t, the following non-dimensional variables for time (τ), radius of wetted bulb (ρ) and depth of water in the pipe (δ) can be derived:

$$\tau = \frac{8K_s t}{\pi^2 r_o},\ \rho = \frac{R}{r_o},\ \partial = \frac{3h}{r_o \Delta\theta}, \tag{1}$$

Where h is the height of water in the permeameter and $\Delta\theta$ is the difference between final and initial volumetric soil moisture content.

$$\text{then, } \frac{d\tau}{d\rho} = \frac{3\rho(\rho-1)}{a^3-\rho^3} \tag{2}$$

Where a is a parameter accounting for soil and permeameter characteristics:

$$a^3 = \frac{3(h_o + \Psi_f + \pi^2 r_o/8)}{r_o \Delta\theta} + 1 \tag{3}$$

Where h_o is the initial height of the water and ψ_f is the suction at the wetting front according to the Green and Ampt equation.

Integrating Eq. (3) for initial conditions $\rho = 1$ for $\tau = 0$ yields the variation of wetted radius Eq. (4) and water depth Eq. (5) with time, respectively:

$$\tau = \left(1 + \frac{1}{2a}\right) ln\left(\frac{a^3-1}{a^3-\rho^3}\right) - \frac{3}{2a} ln\left(\frac{a-1}{a-\rho}\right) + \frac{\sqrt{3}}{a} \arctan\left(\frac{a(\rho-1)\sqrt{3}}{2a^2 + (\rho+1)a + 2\rho}\right) \tag{4}$$

$$\delta = \delta_o - \left(\rho^3 - 1\right) \tag{5}$$

Where δ_o is calculated from Eq. (1) for $h = h_o$.

Please cite this article as: Gwenzi, W., et al., Field-scale spatial variability of saturated hydraulic conductivity on a recently constructed artificial ecosystem, Geoderma (2011), doi:10.1016/j.geoderma.2011.06.010

Philip (1993) proposed the use of two measured times to solve these equations: time required for the water level to reach the midpoint (t_{med}) and time to empty the tube (t_{max}). To avoid the need to estimate ψ_f, the above problem can also be solved in terms of three measured values ($\Delta\theta$, t_{med} and t_{max}). The problem is solved by finding the root a that satisfies the non-linear function:

$$\frac{\tau_{max}}{\tau_{med}} = \frac{t_{max}}{t_{med}} \Rightarrow f(a) = \frac{\tau_{max}}{\tau_{med}} - \frac{t_{max}}{t_{med}} = 0 \tag{6}$$

Where τ_{med} and τ_{max} are calculated from Eq. (4) by setting ρ to ρ_{med} and ρ_{max}, respectively, as given by Eq. (5).

Muñoz-Carpena et al. (2001) developed a computer program that finds a root of Eq. (6). This robust root finding algorithm requires an initial range of a to conduct the search. The upper limit ($a=20$) was chosen as a value higher than the ones calculated from characteristic properties for a range of soil textures. Since $\psi_f>0$, from Eq. (3) the lower limit for a is given by:

$$a > \left(1 + \delta_o + \frac{3\pi^2}{8\Delta\theta}\right)^{1/3} = \left(\rho_{max}^3 + \frac{3\pi^2}{8\Delta\theta}\right)^{1/3} > \rho_{max} \tag{7}$$

If the root found is outside the given boundaries it was considered ill-behaved and the data point is rejected.

Saturated hydraulic conductivity (K_s) was then calculated as:

$$K_s = \left(\frac{\pi^2 r_o \tau_{max}(a)}{8 t_{max}}\right) \tag{8}$$

References

Addinsoft, 2009. XLSTAT Version 2010. Available online www.xlstat.com Addinsoft USA, New York.

Albright, W.H., Benson, C.H., Gee, G.W., Abichou, T., Tyler, S.W., Rock, S.A., 2006. Field performance of three compacted clay landfill covers. Vadose Zone Journal 5, 1157–1171.

Bagarello, V., 1997. Influence of well preparation on field-saturated hydraulic conductivity measured with the Guelph Permeameter. Geoderma 80, 169–180.

Bennett, R.H., Hulbert, M.H., Curry, C., Johnson, H.P., Hutnak, M., Curry, K., 2002. In situ permeabilities of selected coastal marine sediments. IEEE Journal of Oceanic Engineering 27, 571–580.

Blake, G.R., Hartge, K.H., 1986. Bulk density, In: Klute, A. (Ed.), Methods of Soil Analysis Part 1 ASA Monograph No. 9, 2nd ed. Madison, Wisconsin, pp. 363–376.

Bohnhoff, G.L., Ogorzalek, A.S., Benson, C.H., Shackelford, C.D., Apiwantragoon, P., 2009. Field data and water-balance predictions for a monolithic cover in a semiarid climate. Journal of Geotechnical and Geoenvironmental Engineering 135 (3), 333–348.

Bormann, H., Klaassen, K., 2008. Seasonal and land use dependent variability of soil hydraulic and soil hydrological properties of two Northern German soils. Georderma 145, 295–302.

Botros, F.E., Harter, T., Onsoy, Y.S., Tuli, A., Hopmans, J.W., 2009. Spatial variability of hydraulic properties and sediment characteristics in a deep alluvial unsaturated zone. Vadose Zone Journal 8 (2), 276–289.

Bradbury, K.R., Muldoon, M.A., 1990. Hydraulic conductivity determinations in unlithified glacial and fluvial materials. In: Nielson, D.M., Johnson, A.I. (Eds.), Ground Water and Vadose Zone Monitoring. American Society for Testing and Materials (ASTM). Special Technical Publication STP 1053, ASTM, Philadelphia, PA, pp. 138–151.

Breshears, D.D., Nyhan, J.W., Davenport, D.W., 2005. Ecohydrology monitoring and excavation of semiarid landfill covers a decade after installation. Vadose Zone Journal 4, 798–810.

Buczko, U., Gerke, H.H., 2005. Estimating spatial distributions of hydraulic parameters for a two-scale structured heterogeneous lignitic mine soil. Journal of Hydrology 312, 109–124.

Buczko, U., Gerke, H.H., Hüttl, R.F., 2001. Spatial distributions of lignite mine spoil properties for simulating 2-D variably saturated flow and transport. Ecological Engineering 17, 103–114.

Cambardella, C.A., Moorman, T.B., Novak, J.M., Parkin, T.B., Karlen, D.L., Turco, R.F., Konopka, A., 1994. Field-scale variability of soil properties in central Iowa soils. Soil Science Society of America Journal 58, 1501–1511.

Cosby, B.J., Hornberger, G.M., Clapp, R.B., Ginn, T.R., 1984. A statistical exploration of soil moisture characteristics to the physical properties of soils. Water Resources Research 20, 682–690.

Courtney, R.G., Timpson, J.P., 2005. Reclamation of fine fraction bauxite processing residue (red mud) amended with coarse fraction residue and gypsum. Water, Air, and Soil Pollution 164, 91–102.

Dane, J.H., Puckett, W., 1994. Field soil hydraulic properties based on physical and mineralogical information. In: van Genuchten, M.Th., et al. (Ed.), Proceedings of the International Workshop on Indirect Methods for Estimating the Hydraulic Properties of Unsaturated Soils. University of California, Riverside, pp. 389–403.

Deutsch, C.V., Journel, A.G., 1998. GSLIB: Geostatistical Software Library and User's Guide, 2nd edition. Oxford University Press, New York. 369 pp.

Dikinya, O., Hinz, C., Aylmore, G., 2008. Decrease in hydraulic conductivity and particle release associated with self-filtration in saturated columns. Geoderma 146, 192–200.

Eastham, J., Morald, T., Aylmore, P., 2006. Effective nutrient sources for plant growth on bauxite residue. Water, Air, and Soil Pollution 176, 5–19.

Ettema, C.H., Wardle, D.A., 2002. Spatial soil ecology. Trends in Ecology & Evolution 17 (4), 177–183.

Forster, S., Bobertz, B., Bohling, B., 2003. Permeability of sands in the coastal areas of the southern Baltic Sea: mapping a grain-size related sediment property. Aquatic Chemistry 9, 171–190.

Gee, G.W., Bauder, J.W., 1986. Particle size analysis, In: Klute, A. (Ed.), Methods of Soil Analysis, Part 1. Physical and Mineralogical Methods, 2nd Edn. ASA SSSA, Madison, WI, pp. 383–411.

Gerwin, W., Schaaf, W., Biemelt, D., Fischer, A., Winter, S., Hüttl, R.F., 2009. The artificial catchment "Chicken Creek" (Lusatia, Germany) — a landscape laboratory for interdisciplinary studies of initial ecosystem development. Ecological Engineering 35, 1786–1796.

Gherardi, M.J., Rengel, Z., 2001. Bauxite residue sand has the capacity to rapidly decrease availability of added manganese. Plant and Soil 234, 143–151.

Gómez, J.A., Vanderlinden, K., Nearing, M.A., 2005. Spatial variability of surface roughness and hydraulic conductivity after disk tillage: implications for runoff variability. Journal of Hydrology 311, 143–156.

Gwenzi, W., Veneklaas, E., Holmes, K., Bleby, T.M., Ian, Phillips, Hinz, C., 2011. Spatial analysis of root distribution on a recently constructed ecosystem in a water-limited environment. Plant and Soil. doi:10.1007/s11104-011-0744-8.

Gwenzi, W., 2010. Vegetation and soil controls on water redistribution on recently constructed ecosystems in water-limited environments. PhD thesis, The University of Western Australia, Perth.

Holländer, H.M., Blume, T., Bormann, H., Buytaert, W., Chirico, G.B., Exbrayat, J.-F., Gustafsson, D., Hölzel, H., Kraft, P., Stamm, C., Stoll, S., Blöschl, G., Flühler, H., 2009. Comparative predictions of discharge from an artificial catchment (Chicken Creek) using sparse data. Hydrology and Earth System Sciences 13, 2069–2094.

Klaassen, K., Bormann, H., Klenke, T., Liebezeit, G., 2008. The impact of hydrodynamics and texture on the infiltration of rain and marine waters into sand bank island sediments — aspects of infiltration and groundwater dynamics. Senckenbergiana maritima 38 (2), 163–171.

Klute, A., Dirksen, C., 1986. Hydraulic conductivity and diffusivity: laboratory methods, In: Klute, A. (Ed.), Methods of Soil Analysis, Part 1. Physical and Mineralogical Methods, 2nd Edition. ASA SSSA, Madison, WI, pp. 687–734.

Jabro, J.D., 1992. Estimation of saturated hydraulic conductivity of soils from particle size distribution and bulk density data. Transactions of ASAE 35 (2), 557–560.

Johnston, S.G., Hirst, P., Slavich, P.G., Bush, R.T., Aaso, T., 2009. Saturated hydraulic conductivity of sulphuric horizons in coastal floodplain acid sulphate soils: variability and implications. Geoderma 151, 387–394.

Latham, J.P., Munjiza, A., Lu, Y., 2002. On the prediction of void porosity and packing of rock particulates. Powder Technology 125 (1), 10–27.

Mazur, K., Schoenheinz, D., Biemelt, D., Schaaf, W., Grünewald, U., 2011. Observation of hydrological processes and structures in the artificial Chicken Creek catchment. Physics and Chemistry of the Earth 36, 74–86.

Muñoz-Carpena, R., Álvarez-Benedí, J., 2002. Program PDunne. Available online at 2002, University of Florida (USA) and S.I.D.T.A-Valladolid (Spain). http://carpena.ifas.ufl.edu/software/PDunne.htm. Downloaded on 25 June 2008.

Muñoz-Carpena, R., Regalado, C.M., Álvarez-Benedí, J., 2001. The Philip–Dunne permeameter: a low-tech/low-cost filed saturated hydraulic conductivity device. 30 July–1 August 2001 American Society of Agricultural Engineers Annual International Meeting. Sacramento Convention Centre, Sacramento, California, USA.

Muñoz-Carpena, R., Regalado, C.M., Álvarez-Benedí, J., Bartoli, F., 2002. Field evaluation of the new Philip–Dunne permeameter for measuring saturated hydraulic conductivity. Soil Science 167 (1), 9–24.

Ogorzalek, A.S., Bohnhoff, G.L., Shackelford, C.D., Benson, C.H., Apiwantragoon, P., 2008. Comparison of field data and water-balance predictions for a capillary barrier cover. Journal of Geotechnical and Geoengineering 134 (4), 470–486.

Philip, J.R., 1993. Approximate analysis of falling head lined borehole permeameter. Water Resources Research 29, 3763–3768.

Puckett, W.E., Dane, J.H., Hajek, B.H., 1985. Physical and mineralogical data to determine soil hydraulic properties. Soil Science Society of American Journal 49, 831–836.

Reynolds, W.D., Bowman, B.T., Brunke, R.R., Drury, C.F., Tan, C.S., 2000. Comparison of tension infiltrometer, pressure infiltrometer, and soil core estimates of saturated hydraulic conductivity. Soil Science Society of America Journal 64, 478–484.

Reynolds, W.D., Elrick, D.E., 2002. Constant head well permeameter (vadose zone). In: Dane, J.H., Topp, G.C. (Eds.), Methods of Soil Analysis, Part 4. Physical methods. Soil Science Society of America, Inc., Madison, WI, pp. 844–858.

Reynolds, W.D., Elrick, D.E., Young, E.G., Amoozegar, A., Booltink, H.W.G., Bouma, J., 2002. Saturated and field-saturated water flow parameters. In: Dane, J.H., Topp, G.C. (Eds.), Methods of Soil Analysis, Part 4, Physical Methods. Soil Science Society of America, Inc., Madison, WI, pp. 797–878.

Please cite this article as: Gwenzi, W., et al., Field-scale spatial variability of saturated hydraulic conductivity on a recently constructed artificial ecosystem, Geoderma (2011), doi:10.1016/j.geoderma.2011.06.010

Saxton, K.E., Rawls, W.L., Rosenberger, J.S., Papendick, R.I., 1986. Estimating generalized soil–water characteristics from texture. Soil Science Society of America Journal 50, 1031–1238.

Sobieraj, J.A., Elsenbeer, H., Coelho, R.M., Newton, B., 2002. Spatial variability of soil hydraulic conductivity along a tropical rainforest catena. Geoderma 108, 79–90.

Sobieraj, J.A., Elsenbeer, H., Vertessy, R.A., 2001. Pedotransfer functions for estimating saturated hydraulic conductivity: implications for modeling storm flow generation. Journal of Hydrology 251, 202–220.

Swanson, D.A., Barbour, S.L., Wilson, G.W., O'Kane, M., 2003. Soil–atmosphere modelling of an engineered soil cover for acid generating mine waste in a humid, alpine climate. Canadian Geotechnical Journal 40, 276–292.

Tietje, O., Hennings, V., 1996. Accuracy of the saturated hydraulic conductivity prediction by pedotransfer functions compared to the variability within FAO textural classes. Geoderma 69, 71–84.

van Genuchten,, M.Th., Leij, F.J., Yates, S.R., 1991. The RETC code for quantifying the hydraulic functions of unsaturated soils. Version 6.02 EPA Report 600/2-91/065. U.S. Salinity Laboratory, USDA, ARS, Riverside, California (Available on-line http://www.pc-progress.com/en/Default.aspx?RETC.

Wang, T., Zlotnik, V., Šimunek, J. And, Schaap, M., 2009. Using pedotransfer functions in vadose zone models for estimating groundwater recharge in semiarid regions. Water Resources Research 45, W04412. doi:10.1029/2008WR006903.

Webb, G., Tyler, S.W., Collord, J., Van Zyl, D., Halihan, T., Turrentine, J., Fenstemaker, T., 2008. Field-scale analysis of flow mechanisms in highly heterogeneous mining media. Vadose Zone Journal 7, 899–908.

Wehr, J.B., So, H.B., Menzies, N.W., Fulton, I., 2005. Hydraulic properties of layered soils influence survival of Rhodes grass (*Chloris gayana* Kunth.) during water stress. Plant and Soil 270, 287–297.

Wiebenga, W.A., Ellis, W.R., Kevi, L., 1970. Empirical relations in properties of unconsolidated quartz sands and silts pertaining to water flow. Water Resources Research 6, 1154–1161.

Wilson, A.M., Huettel, M., Klein, S., 2008. Grain size and depositional environment as predictors of permeability in coastal marine sands. Estuarine, Coastal and Shelf Science 80, 193–199.

Woodard, H.J., Hossner, L., Bush, J., 2008. Ameliorating caustic properties of aluminium extraction residue to establish a vegetative cover. Journal of Environmental Science and Health, Part A 43, 1157–1166.

Zhang, Z.F., Groenevelt, P.H., Parkin, G.W., 1998. The well shape-factor for the measurement of soil hydraulic properties using the Guelph Permeameter. Soil and Tillage Research 49, 219–221.

Zhu, J., Mohanty, B.P., 2002. Spatial averaging of van Genuchten hydraulic parameters for steady-state flow in heterogeneous soils: a numerical study. Vadose Zone Journal 1, 261–272.

Please cite this article as: Gwenzi, W., et al., Field-scale spatial variability of saturated hydraulic conductivity on a recently constructed artificial ecosystem, Geoderma (2011), doi:10.1016/j.geoderma.2011.06.010